



- 1 National-Scale Inventory based Climate Impact Analysis of the Nitrogen Balance, including all Nitrogen
- 2 Fluxes using Process-Based Modelling with the LandscapeDNDC Model and EURO-CORDEX Ensembles
- 3 for Greece
- 4
- 5 Odysseas Sifounakis<sup>1</sup>, Edwin Haas<sup>2,\*</sup>, Klaus Butterbach-Bahl<sup>2,3</sup>, Eleni Katragkou<sup>4</sup>, Maria Chara Karypidou<sup>4,5</sup>
- 6 and Maria P. Papadopoulou<sup>1</sup>
- 7 1 Laboratory of Physical Geography and Environmental Impacts, School of Rural, Surveying and
- 8 Geoinformatics Engineering, National Technical University of Athens, Athens, 15780, Greece
- 9 <sup>2</sup> Institute of Meteorology and Climate Research (IMK-IFU), Karlsruhe Institute of Technology (KIT),
- 10 Kreuzeckbahnstr. 19, D-82467 Garmisch-Partenkirchen, Germany
- 11 3 Department of Agroecology Center for Landscape Research in Sustainable Agricultural Futures Land-
- 12 CRAFT, Aarhus University, Aarhus, 8000, Denmark
- 13 <sup>4</sup> Aristotle University of Thessaloniki, Department of Meteorology and Climatology, School of Geology,
- 14 Aristotle University of Thessaloniki, Greece
- 15 Institute of Climate and Atmospheric Science, School of Earth and Environment, University of Leeds, UK
- 17 \*Correspondence to: Edwin Haas (edwin.haas@kit.edu)
- 19 Keywords: arable land, greenhouse gase, ensemble modelling, crop model, food security

# 21 Abstract

16

18

- 22 In this study, we have simulated inventories of arable production and soil carbon and nitrogen cycling on
- 23 a national scale (0.25 x 0.25-degree) for Greece with the bio-geochemical ecosystem model
- 24 LandscapeDNDC. Based on observation data, we have aggregated for each grid cell 4 most likely crop
- 25 rotations, including nitrogen and manure fertilization, tilling and irrigation. The arable management was
- 26 continuously projected into the future until 2100, while plant phenology was adapted to local conditions,
- 27 general properties of the arable management were kept constant into the future, such as the selection of
- 28 crops or the share of irrigated arable land. To understand the impacts of climate change, we used the
- 29 EURO-CORDEX-11 regional climate ensemble to drive the LandscapeDNDC impact model under scenarios
- 30 RCP4.5 (16 datasets) and RCP8.5 (32 datasets). The simulation timespan was from 1990 until 2100, using
- 31 the first 10 years as spin-up to obtain equilibrium in the model's internal carbon and nitrogen pools from
- 32 the model initialization.
- 33 Arable production declines from 2045 onwards by 9.5% or 144 kg C ha<sup>-1</sup> yr<sup>-1</sup> under RCP4.5 and by 29% or
- 484 kg C ha<sup>-1</sup> yr<sup>-1</sup> towards 2100. At present, the ensemble results show an average soil carbon loss of 122.1
- kg C ha<sup>-1</sup> yr-1 versus 139.7 kg C ha<sup>-1</sup> yr<sup>-1</sup> in the future. The gaseous outfluxes of the ensemble simulations
- 36 show  $N_2O$  emissions of 0.494 to 0.453 kg  $N_2O-N$  ha<sup>-1</sup> yr<sup>-1</sup>, NO emissions of 0.031 kg NO-N ha<sup>-1</sup> yr<sup>-1</sup>,  $N_2$

# https://doi.org/10.5194/egusphere-2025-5311 Preprint. Discussion started: 2 December 2025 © Author(s) 2025. CC BY 4.0 License.





emissions of 4.806 to 3.377 kg N<sub>2</sub>–N ha<sup>-1</sup> yr<sup>-1</sup>, NH<sub>3</sub> emissions of 24.662 to 35.040 or 34.205 kg NH<sub>3</sub>–N
ha<sup>-1</sup> yr<sup>-1</sup> and nitrate leaching losses from 54.304 to 58.213 kg NO<sub>3</sub>-N ha<sup>-1</sup> yr<sup>-1</sup> comparing present versus
future conditions. The overall nitrogen balance of the ensemble simulations reveals a mean nitrogen loss
of 4.7 versus 5.7 kg-N ha<sup>-1</sup> yr<sup>-1</sup> comparing present to future conditions.





#### Highlights 42

- 43 21st century temperature increase of 1.37°C under RCP4.5 and 3.21°C under RCP8.5 from the ensembles 44
  - Precipitation decreases of 17.96 mm for RCP4.5 and 102.52 mm under RCP8.5 from the ensembles
  - Arable production decreases by 9.5% under RCP4.5 and by 29% under RCP8.5
  - Ensemble results show a soil carbon loss of 122.1 under RCP4.5 versus 139.7 kg C ha<sup>-1</sup> yr<sup>-1</sup> under RCP8.5
  - Ensemble simulations show averaged N<sub>2</sub>O emissions of 0.494 for RCP4.5 and 0.453 kg N<sub>2</sub>O-N ha<sup>-1</sup> yr<sup>-1</sup> under RCP8.5

52 53

45

46 47

48

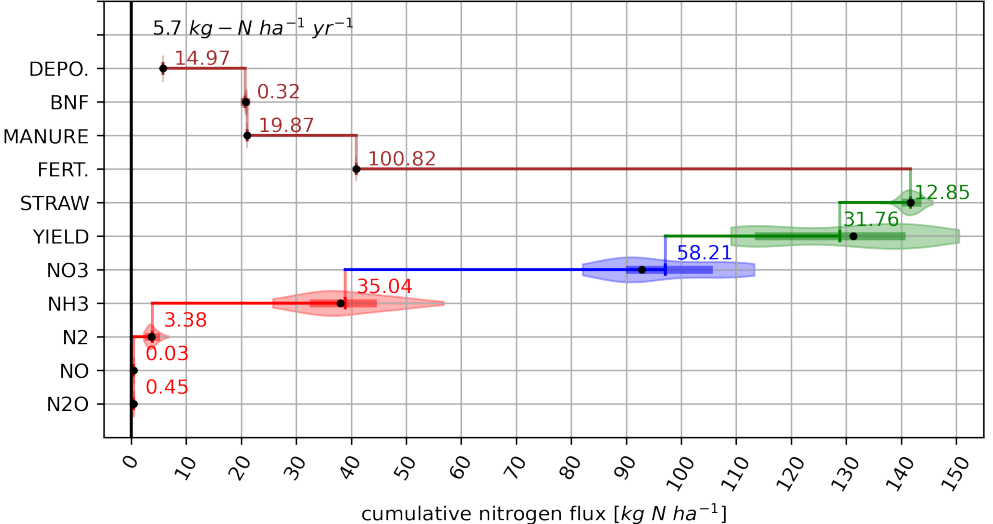
49

50 51

# **Graphical abstract**

54 55

# Cumulative nitrogen balance RCP85, average 2080-2100



56 57

61

62 63

64

65

66

67 68

69

70

71

72

73

74

75 76

77

78

79

80

81

82

83

84

85

86

87

88

89

90

91

92

93

94

95

the carbon and nitrogen modeling.





## 1 Introduction

In a rapidly changing global climate, the intricate relationships within agroecosystems among crop production, biogeochemical cycles, and greenhouse gas emissions have emerged as focal points of scientific research. It also affects food security via direct and indirect effects such as agricultural productivity, e.g., via elevated atmospheric CO<sub>2</sub> concentrations, but also soil nutrient cycles, driven largely by increasing temperature trends but also extreme temperature exposures, altered precipitation regimes, drought patterns, and erosion, carbon nitrogen depletion, etc. Uncertainties related to the evolution of future socioeconomic pathways (SSP) and scientific uncertainties related to the incomplete knowledge of climate and agroclimatic processes contribute to the cascade of uncertainty in all climate impact studies and risk assessments (see Fig. 1 of Wilby & Dessai, 2010). While our general understanding of these changes is high on a global level, the level of confidence in these projections varies from regional to local levels. Giorgi, (2006) reported the Mediterranean as a vulnerable region worldwide due to its high exposure to the effects of climate. The area is characterized by a high population density and high socioeconomic importance, as it sustains a large proportion of the European Food Production System. General circulation models (GCMs) have been extensively used in the past to assess the changes in the state of climate, providing large-scale information on essential climate variables (Bojinski et al., 2014), although their spatial resolution is generally low (Nocentini et al., 2015; Yang & Villarini, 2021). Regional climate models (RCMs) can be used to enhance the spatial and temporal resolution of the GCM projections by conducting dynamical downscaling from a regional to a national level (Giorgi, 2006). Selecting a specific GCM/RCM model combination for a specific region for a climate projection may still be biased due to systematic model behaviors, possibly originating from either or both the GCM and the RCM (Eden et al., 2012) models. Therefore, it is advisable to use an ensemble of GCM/RCM climate projections to assess the climate change impact on a regional to local scale (Paeth et al., 2023). While the approach of propagating ensembles of climate projections through models has already been used, e.g., in hydrology (Weiland et al., 2021) it has not been addressed with ecosystem models on the national scale, and studies addressing the full nitrogen balance are still very limited (Petersen et al., 2021); example of grassland on a local scale, and additionally examples of climate impact assessments with ensembles, full N balance in Austria (Schroeck et al., 2019), and Thessaly, an example in Greece by Sifounakis et al., (2024). In this study, we aim to present national-scale assessments of the full nitrogen and carbon balance, including all associated fluxes of reactive and non-reactive nitrogen (such as NO, N2, N2O, NH3 emissions, NO₃ leaching, N-in-yield, biological nitrogen fixation) of the cropland cultivation for Greece for present and future conditions on a national scale. Besides the aforementioned, we also investigated the uncertainty due to climate change projections on

# https://doi.org/10.5194/egusphere-2025-5311 Preprint. Discussion started: 2 December 2025 © Author(s) 2025. CC BY 4.0 License.





96	To obtain these results, we propagated the European climate dataset of the Coordinated Regional Climate
97	Downscaling Experiment (EURO-CORDEX) (Jacob et al., 2020) under the mid-impact and high-impact
98	Representative Concentration Pathway scenarios (RCP4.5 and RCP8.5, respectively) through the
99	LandscapeDNDC model to compile result ensembles of detailed inventory simulations.
100	The following research questions are addressed in the study:
101	a) Assessment of the full nitrogen balance of the Greek cropland system for present conditions as
	, , , , , , , , , , , , , , , , , , , ,
102	demanded by UN FCCC reporting
103	b) Climate change impact analysis on agricultural production on a national scale due to climate
104	change projections
105	c) Assessment of the soil carbon balance of the agricultural cropland system for present conditions
106	and future projections under climate change
107	d) Climate change impact analysis on the carbon and nitrogen cycle and fluxes towards 2100
108	The novelty of the study is the use of process-based modelling on a national scale for the first time to
109	address questions a) to d).



111

139

140

141

142



## 2 Material and Methods

# 2.1 Biogeochemical Model

112 Biogeochemical models, such as LandscapeDNDC (Haas et al., 2013), simulate the processes of carbon and 113 nitrogen cycling in croplands based on model initialization with soil physical and chemical properties. Agricultural management and climate data need to be provided as boundary conditions to drive the model 114 115 simulations forward in time. 116 LandscapeDNDC (Haas et al., 2013) is a modular, process-based ecosystem model designed to simulate 117 biogeochemical changes in carbon (C) and nitrogen (N) within croplands, forests, and grasslands at both 118 site-specific and regional scales. It integrates various modules related to plant growth, micro-119 meteorology, water cycling, as well as physico-chemical, plant, and microbial C and N cycling. Additionally, it models interactions between terrestrial ecosystems and the atmosphere and hydrosphere. 120 121 LandscapeDNDC is a generalized framework for plant development and soil biogeochemistry, built upon 122 the foundations of agricultural DNDC and Forest-DNDC models (Li, 2000). The model has been used and 123 tested for Greek conditions in a previous study by Sifounakis et al. (2024) and was deployed in the same 124 125 To initialize LandscapeDNDC, site-specific physical and chemical soil profile data are utilized, including 126 information at different soil depths. This data includes soil organic carbon (SOC) and nitrogen (SON) content, soil texture (proportions of clay, sand, and silt), bulk density, pH levels, saturated hydraulic 127 128 conductivity, field capacity, and wilting point. Additionally, the model incorporates daily or hourly climate 129 variables such as air temperature (maximum, minimum, and average), precipitation, solar radiation, air 130 chemistry data related to dry and wet nitrogen deposition, and atmospheric CO₂ concentration. 131 Agricultural management practices, such as crop planting and harvesting, fertilization (both organic and 132 synthetic), feed cutting, and tilling, are also integrated to drive LandscapeDNDC simulations. Crop growth 133 is modeled using a temperature degree sum approach, incorporating CO2 concentrations, while daily growth limitations due to water and nutrient availability, as well as drought stress, are also considered. 134 135 In this study, site-specific crop parameterizations were derived from a previous study by Sifounakis et al., 136 (2024). A detailed overview of the cultivated crops, crop rotations, fertilization practices, and manure 137 application is provided in Fehler! Verweisquelle konnte nicht gefunden werden. (supplementary 138 material).

# 2.2 National scale model input data

The national-scale input data sets for this modelling study were extracted from a previous study by Haas et al. (2022). The dataset decomposed Greece into 430 conformal 0.25° latitude x 0.25° longitude grid cells, each holding, e.g., profile information of soil physical and chemical properties for model initialization





based on the European Soil Database (ESDB, 2004). The grid cells were assigned their share of arable land based on the aggregation of Corine Landcover data, which assigned the diverse Greek land use into 3 major agricultural classes: arable land, grassland, and forests. The resulting arable land class containing 2.9 mio ha consists of cultivated agricultural (1.6 mio ha), agroforestry/tree plantations (1.0 mio ha), vineyards (0.1 mio ha), and the rest (fallow land, gardens, 0.2 mio ha) (ELSTAT: https://www.statistics.gr/en/statistics/-/publication/SPG06/2023, last access: February 2024).

## 2.2.1 Agricultural management

Agricultural management data to drive model simulations was available from Haas et al. (2022) for the period 1951-2100. For this study, we have aggregated this management data to the simulation period 1990-2100, while the period 1990-2005 was used as a prerun period to achieve equilibrium for the soil carbon and nitrogen pools, and the evaluation period 2005-2100 was used for the climate impact assessment.

Synthetic fertilizer input originates from FAO statistics, and manure use was assessed from regional statistics of animal head numbers for main livestock classes (data adapted from Haas et al., 2022). The arable land was divided into rainfed and irrigated land according to Mirca 2000 (Portmann et al., 2010) and national reports as used by (Sifounakis et al., 2024). Mirca lacks a projection of irrigation use

2010) and national reports as used by (Sifounakis et al., 2024). Mirca lacks a projection of irrigation use into the future; thus, the assumptions on irrigation management were kept constant in this study. On a national scale, the share of rainfed versus irrigated cropland cultivation was 52/48 % (Sifounakis et al., 2024).

# 2.2.2 EURO-CORDEX regional climate data

In this study, we retrieve regional climate data from the EURO-CORDEX data repositories, with a spatial resolution of  $^{\sim}$  12 Km (0.11°). The various combinations of GCMs/RCMs are shown in Table 1. The 16/32 model combinations consist of 6 GCMs, as well as 8 RCMs, comprising structural variability/uncertainty of climate change projections until 2100. The two climate change ensembles represent only subsets of the EURO-CORDEX ensembles. The EURO-CORDEX ensembles consist of more climate change projections, but due to constraints in data availability for download from the various data centers/repositories and completeness for all necessary variables, we had to limit the study to the climate change projections summarized in Table 1 at the start of this study. Note that 14 GCM/RCM combinations are common in both RCPs, while the RCP4.5 ensemble contains 2 unique combinations not present in the RCP8.5, and the RCP8.5 ensemble contains 18 unique combinations not present in the RCP4.5 ensemble.

the simulation grid. The interpolated variables used to drive the LandscapeDNDC model were daily

# https://doi.org/10.5194/egusphere-2025-5311 Preprint. Discussion started: 2 December 2025 © Author(s) 2025. CC BY 4.0 License.





- averaged temperature (tas), daily maximum temperature (tasmax), daily minimum temperature (tasmin),
- shortwave down global radiation (rsds), and precipitation flux (pr).





Table 1. Climate datasets obtained for the current study from EURO-CORDEX for medium (16 representations for RCP4.5) and extreme scenarios (32 representations for RCP8.5), respectively. The datasets consist of a historical period (1951-2004) and the future climate change projection time spans (2005-2100). 14 GCM-RCM combinations are common in both RCPs, while RCP4.5 ensemble contains 2 unique combinations, and the RCP8.5 ensemble contains 18 unique combinations. <sup>1)</sup> global circulation model, <sup>2)</sup> regional climate model (for details, see Olschewski et al., 2024).

No.	Scenario	GCM <sup>1)</sup>	RCM <sup>2)</sup>	common / unique
1	RCP4.5	CNRM-CERFACS-CNRM-CM5	CLMcom-CCLM4-8-17	common
2	ICI 4.5	CIVILIVI CEITI ACS CIVILIVI CIVIS	KNMI-RACMO22E	common
3			SMHI-RCA4	common
4		ICHEC-EC-EARTH	CLMcom-CCLM4-8-17	common
5		ICHEC-EC-EARTH	KNMI-RACMO22E	common
6			SMHI-RCA4	common
7		IPSL-CM5A-MR	SMHI-RCA4	common
8		MOHC-HadGEM2-ES	CLMcom-CCLM4-8-17	common
9		WOTIE-HAUGEWIZ-E3	DMI-HIRHAM5	
10			KNMI-RACMO22E	unique
11		MPI-ESM-LR	CLMcom-CCLM4-8-17	common
12		IVIPI-ESIVI-LK	SMHI-RCA4	common
13			MPI-CSC-REMO2009	common
		NCC No. FCN41 NA		common
14		NCC-NorESM1-M	DMI-HIRHAM5	unique
15			SMHI-RCA4	common
16			GERICS-REMO2015	common
1	RCP8.5	CNRM-CERFACS-CNRM-CM5	CLMcom-CCLM4-8-17	common
2			CLMcom-ETH-COSMO-	unique
			crCLIM-v1-1	
3			DMI-HIRHAM5	unique
4			KNMI-RACMO22E	common
5			SMHI-RCA4	common
6			GERICS-REMO2015	unique
7			ICTP-RegCM4-6	unique
8		ICHEC-EC-EARTH	CLMcom-CCLM4-8-17	common
9			CLMcom-ETH-COSMO-	unique
			crCLIM-v1-1	
10			DMI-HIRHAM5	unique
11			KNMI-RACMO22E	common
12			SMHI-RCA4	common
13			ICTP-RegCM4-6	unique
14		IPSL-CM5A-MR	DMI-HIRHAM5	unique
15			KNMI-RACMO22E	unique
16			SMHI-RCA4	common
17			GERICS-REMO2015	unique
18		MOC-HadGEM2-ES	CLMcom-CCLM4-8-17	common
19			CLMcom-ETH-COSMO-	unique
			crCLIM-v1-1	
20			KNMI-RACMO22E	common
21			SMHI-RCA4	unique





22	MPI-ESM-LR	CLMcom-CCLM4-8-17	common
23		CLMcom-ETH-COSMO-	unique
		crCLIM-v1-1	
24		DMI-HIRHAM5	unique
25		KNMI-RACMO22E	unique
26		SMHI-RCA4	common
27		MPI-CSC-REMO2009	common
28		ICTP-RegCM4-6	unique
29	NorESM1-M	CLMcom-ETH-COSMO-	unique
		crCLIM-v1-1	
30		KNMI-RACMO22E	unique
31		SMHI-RCA4	common
32		GERICS-REMO2015	common

## 2.3 Climate Change Impact Assessment

Climate data was analysed for grid cells containing arable land over the study region. Thus, grid cells over the sea, neighboring countries, and non-cropland areas/land use (e.g., mountains) were excluded from the analysis.

For the climate impact analysis, we consider the present conditions at 2020, the 30-year time slice from 2005 until 2034, and for future conditions, the time slice from 2070 until 2099. All spatial data aggregations were built using cropland area-weighted aggregations. All figures showing time series were using 10-year rolling means to reduce fluctuations. In general, when comparing model outcomes for the present and future, spatial and temporal means are assumed. These statistics were used and described/analyzed in section 3.4.

The analysis displays the chronological evolution of the carbon and nitrogen cycle components towards the end of the 21<sup>st</sup> century. We further quantify the impact of climate change on these components between current and future conditions.

# 2.3.1 Chronological evolution until the end of the 21st century

The biogeochemical model simulation results were analyzed for the period 2020 - 2100. Aggregation for all output quantities across all ensemble simulations was performed as follows:

- 1. Spatial aggregation: Averaging the country-wide 430 grid cells on a daily resolution, weighted by the share of arable land within each grid cell.
- 2. Temporal aggregation: Averaging or summing up from step 1 to obtain annual values; averages on a national scale were derived by dividing the totals by the total arable land area across all grids to obtain area-weighted average fluxes per hectare.





To assess the climate change impact, statistical analysis was applied across the ensemble time series from the above-mentioned aggregations, resulting in ensemble statistics such as means, medians, standard deviations, and 25- and 75-quartiles. Higher-level quantitative approaches, such as performing statistics on the grid cell basis, as done by Haas et al., (2022) was not considered in this study.

### 3 Results

Simulation of the Greek cropland production system under projected climate change conditions (starting 1990, evaluation 2005-2100) displays distinct temporal and spatial patterns of impact on agricultural production, and carbon and nitrogen cycling dynamics in agricultural soils. The simulations account for increasing atmospheric CO<sub>2</sub> concentration under RCP4.5 and RCP8.5, and shifts in temperature and precipitation dynamics represented by the various regional climate model simulations.

# 3.1 Climate change characteristics of the EURO-CORDEX RCP4.5 and RCP8.5 ensembles

The climatic information provided by the EURO-CORDEX ensemble of simulations over the study region

displays distinct spatio-temporal patterns of climate change, concerning temperature and precipitation. This information is subsequently used in the impact assessment of the LandscapeDNDC model.

The analysis of the climate change prediction ensembles shows for the arable land in Greece, during the 21st century, an average temperature increase of 1.37°C (increase in: ensemble median 1.35, Q25 of 1.43 and Q75 of 1.31 °C) for RCP4.5, and of 3.21°C (increase in: ensemble median 3.30, Q25 of 2.74, Q75 of 3.60°C) for RCP8.5. The standard deviations increase between present and future conditions, reflecting the increase in spread between the ensemble members. The data is shown on Figure 1 (a, c) and summarized in Table 2. For the precipitation dynamics, shown on Figure 1 (b, d), a systematic decrease is expected under both RCPs. More specifically, we see a decrease of 17.96 mm (change in: ensemble median -10.57, Q25 of -45.18, and Q75 of -9.74 mm) for RCP4.5 and a decrease of 102.52 mm (change in: ensemble median -91.05, Q25 of -120.16, and Q75 of -86.20mm) for RCP8.5. The standard deviations for the ensemble precipitation also rise, indicating a greater spread among the ensemble members. From the aforementioned analysis of the EURO-CORDEX ensemble, it becomes evident that the impact of climate change becomes more severe towards the end of the 21st century, and ensemble spread also increases moving away from the current period (towards the end of the 21st). Data is summarized in Table 2.



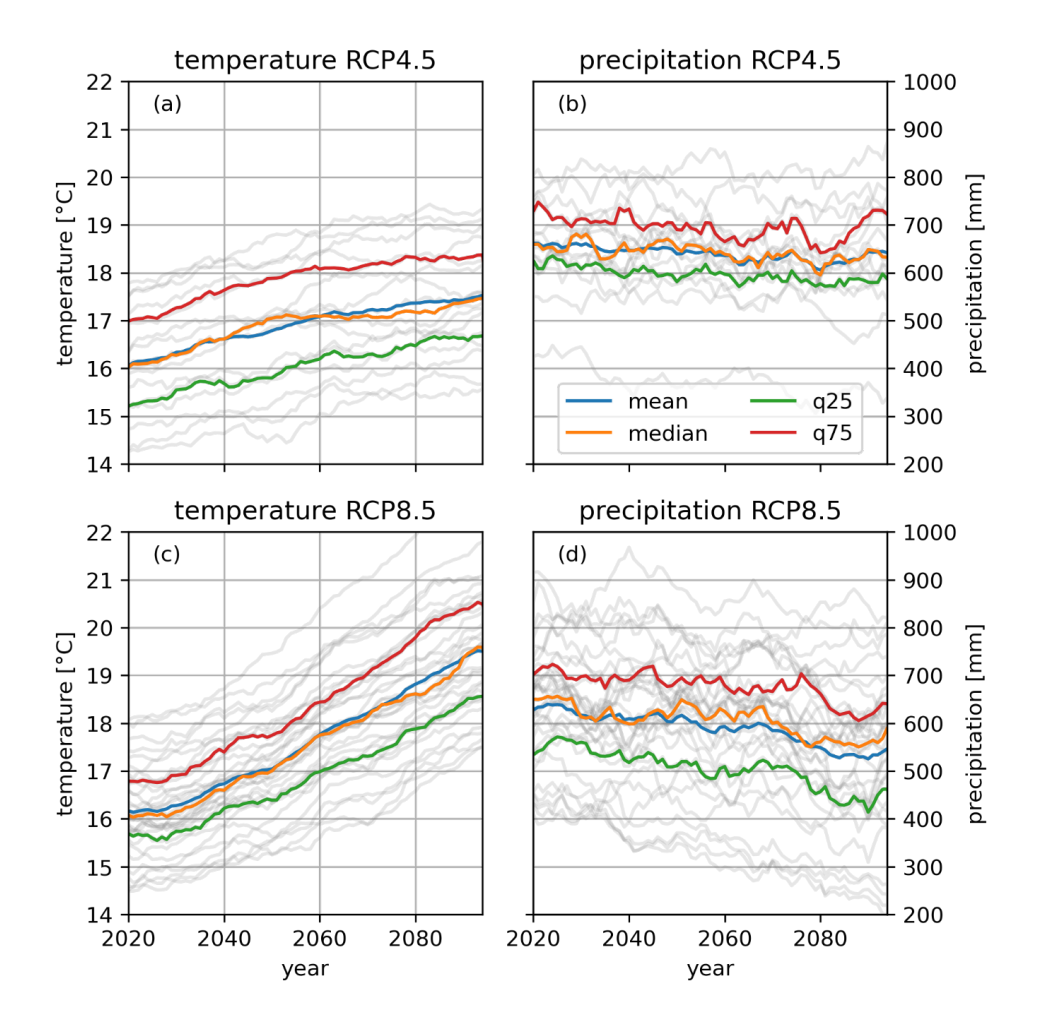


Figure 1. Annual projections of temperatures (a, c), and precipitation (b, d) for arable land in Greece as 10-year rolling means for RCP4.5 (a, b) and RCP8.5 (c, d). Data based on reprojected EURO-CORDEX ensembles considering only grid cells with arable land in Greece (see summary Table 2). Grey lines represent individual ensemble members, blue the mean, orange the median, and green and red the interquartile range.





Table 2. Temperature and precipitation analysis of the climate change ensembles for the present (2005-2035) and future (2070-2100) conditions (30-year periods). Data based on reprojected EURO-CORDEX ensembles (see Table 1) considering only grid cells with arable land in Greece.

		Tempe	rature		Precipitation				
	Present	Future	Change rate		Present	Future Chan		nge rate	
	[°C]	[°C]	[°C]	[%]	[mm]	[mm]	[mm]	[%]	
RCP4.5									
Mean	16.05	17.42	1.37	8.5	661.62	643.66	-17.96	-2.7	
Median	16.03	17.38	1.35	8.4	659.07	648.50	-10.57	-1.6	
Std	1.27	1.37	0.10	7.9	91.08	121.79	30.71	33.7	
Q25	15.21	16.64	1.43	9.4	625.25	580.07	-45.18	-7.2	
Q75	16.99	18.30	1.31	7.7	728.42	718.68	-9.74	-1.3	
RCP8.5									
Mean	16.17	19.38	3.21	19.9	627.86	525.34	-102.52	-16.3	
Median	16.07	19.37	3.30	20.5	650.36	559.31	-91.05	-14.0	
Std	0.97	1.31	0.34	35.1	129.19	158.50	29.31	22.7	
Q25	15.69	18.43	2.74	17.5	534.01	413.85	-120.16	-22.5	
Q75	16.79	20.39	3.60	21.4	701.94	615.74	-86.20	-12.3	

## 3.2 Agricultural production response of major crops

The ensemble response to the climate change scenarios shows different responses for the SSP RCP4.5 and RCP8.5, especially in the second half of the century, when assessing the averaged biomass carbon yield across all various crops within the rotations for the various inventory simulations. Arable production under RCP4.5 remains constant until 2045, followed by a clear decrease towards 2100 on average of 144 kg C ha<sup>-1</sup> yr<sup>-1</sup> (decline of approx. 9.5% compared to present conditions, while medians decrease by 111 kg C ha<sup>-1</sup> yr<sup>-1</sup>), while the spread of the ensemble simulations increases as well towards 2100, indicated by an increase of the standard deviation. Under RCP8.5, arable production dynamics show similar behavior with a much stronger decline after 2045, resulting in substantial yield reductions of 484 kg C ha<sup>-1</sup> yr<sup>-1</sup> (median losses of 544 kg C ha<sup>-1</sup> yr<sup>-1</sup>) corresponding to lower values of approx. 29% and 31% respectively, comparing future to present conditions. Comparing predicted yields for the future time slice, the RCP4.5 scenario shows significantly higher yields (corresponding to smaller losses) compared to the RCP8.5 ensemble.





Considering means, the RCP8.5 ensemble predicts 15% lower production, and even 24% lower yields compared to the RCP4.5 ensemble (see the summary of future predicted arable production in Table 3). For both scenarios, the IQR of the simulated yield ensembles increases from present to the future, for RCP4.5 from 1080 to 1210 versus 612 to 975 kg C ha<sup>-1</sup> yr<sup>-1</sup> for RCP8.5, respectively, which can be seen in Figure 2 and summarized in Table 3. The characteristics of the simulated production ensembles strongly correlate with the ensemble dynamics for temperature and precipitation driving the simulations. Table 3 summarizes all results for the analysis of the simulation ensembles for straw removed from the fields after the harvest.

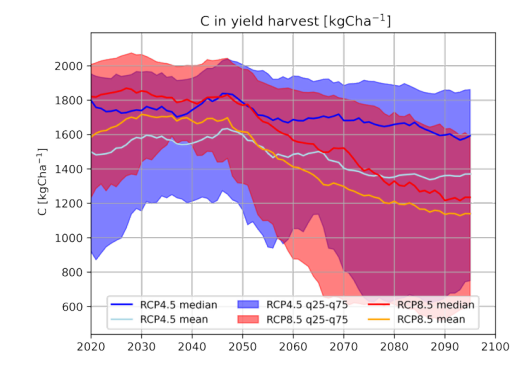


Figure 2. Dynamics of averaged cropland production of the ensembles on the national scale under climate change scenarios (analysis based on yearly area weighted averaged carbon yields across all crops on a national scale).





Table 3. Analysis of arable production (crop yield and straw) of the simulation ensembles under climate change scenarios (present: 2015 – 2034, future 2070 – 2099). Yield and straw are area weighted of all crops across all 430 grid cells.

	arable	e production (y	rields)		straw harvest		
		[kg C ha <sup>-1</sup> yr <sup>-1</sup> ]		[kg C ha <sup>-1</sup> yr <sup>-1</sup> ]			
	Present Future Change rate		Present	Future	Change rate		
RCP4.5							
Mean	1511.7	1367.7	-144.0	1082.2	995.6	-86.6	
Median	1735.9	1624.6	-111.3	1114.8	1027.1	-87.7	
Std	535.9	571.4	35.5	133.2	149.3	16.1	
Q25	862.5	650.2	-212.3	1012.5	889.5	-123.0	
Q75	1942.8	1860.6	-82.2	1175.2	1099.1	-76.1	
RCP8.5							
Mean	1644.9	1161.1	-483.8	1108.4	865.7	-242.7	
Median	1776.8	1233.1	-543.7	1142.0	862.1	-279.8	
Std	471.9	511.2	39.3	161.7	186.3	24.6	
Q25	1394.3	604.3	-790.0	1066.7	723.1	-343.6	
Q75	2006.1	1578.9	-427.2	1199.2	1017.3	-181.9	

# 3.3 Full carbon and nitrogen balance

# 3.3.1 Carbon balance

The ecosystem carbon balance consists of influxes, including GPP (gross primary production, or photosynthesis), and carbon input via manure. The carbon outflux consists of TER (terrestrial ecosystem respiration, encompassing both autotrophs and heterotrophs) and carbon removal via yield harvest. The difference between these two represents the carbon gain or loss of the system. Figure 3 illustrates the carbon fluxes for the different climate change scenarios, including the various carbon fluxes involved. The net carbon flux of the system, i.e., a net carbon loss from the soil, is quantified in Table 3 for both present and future conditions. At present, the RCP4.5 ensemble results in a yearly C loss of 122.1 or 264.9 kg C ha

# https://doi.org/10.5194/egusphere-2025-5311 Preprint. Discussion started: 2 December 2025 © Author(s) 2025. CC BY 4.0 License.

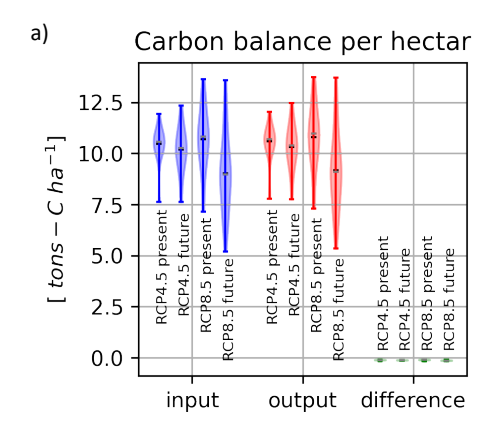




288	<sup>1</sup> yr <sup>-1</sup> , considering the mean versus median, respectively, and 120.6 or 168.1 kg C ha <sup>-1</sup> yr <sup>-1</sup> losses for the
289	$RCP8.5\ ensemble, considering\ the\ mean\ versus\ median,\ respectively.\ For\ the\ future\ time\ slice,\ the\ RCP4.5$
290	ensembles result in yearly C losses of 126.0 or 21.7 and 139.7 or 204.8 kg C ha $^{\text{-}1}$ yr $^{\text{-}1}$ , considering the mean
291	versus median for RCP4.5 versus RCP8.5 (see Table 4).
292	The partitioning of the carbon balance into different carbon fluxes is illustrated in Figure 3 b) and
293	summarized in Table 4. Overall, the impact of climate change on carbon balance displays non-significant
294	changes between the beginning and end of the 21st century in both RCP scenarios.







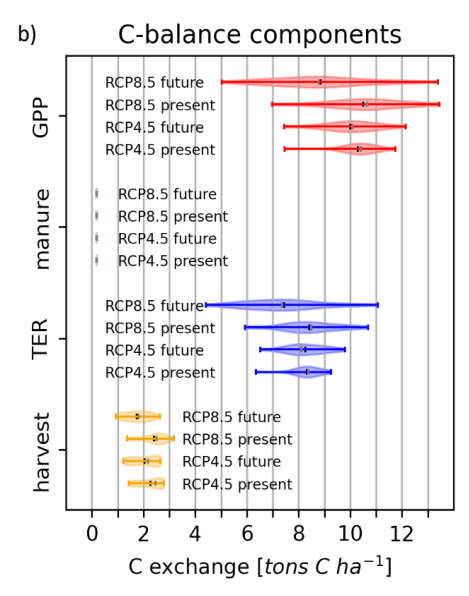


Figure 3. Carbon balance assessment of cropland cultivation in Greece on a national scale for a) input/output/difference and b) the components of the Carbon Balance for RCP4.5 and RCP8.5 and time slices present and future.

298299

296





Table 4. Summary of the carbon balance for present and future conditions for a) RCP4.5 and b) RCP8.5 scenarios. The C input via organic fertilization (manure) remains constant in the study and is therefore not listed.

	Present (2005-2035)			Futu	re (2070-21	Change			
	[kg-C ha <sup>-1</sup> yr <sup>-1</sup> ]			[kg-C ha <sup>-1</sup> yr <sup>-1</sup> ]			[kg-C ha <sup>-1</sup> yr <sup>-1</sup> ]		
	Mean	Std	Median	Mean	Std	Median	Mean	Std	Median
RCP4.5									
GPP	10280.4	893	10395.9	10005.4	1119	10074.7	-275	226	-321.2
C in manure	175	0	175	175	0	175	0	0	0
TER	8313.3	657.8	8372.7	8265.2	811.8	8104	-48.1	153.9	-268.7
C-in-yield	2264.2	477.9	2463.1	2041.2	508.4	2167.4	-223	30.6	-295.7
ΔC flux	-122.1		-264.9	-126		-21.7	-3.9		243.2
RCP8.5									
GPP	10507.7	1540.9	10651.8	8855.2	1937.1	8781	-1652.4	396.2	-1870.8
C in manure	175	0	175	175	0	175	0		0
TER	8405.1	1119.5	8492.1	7428.7	1516.2	7358.5	-976.4	396.7	-1133.6
C-in-yield	2398.2	480.7	2502.8	1741.2	484.7	1802.3	-656.9	4	-700.4
ΔC flux	-120.6		-168.1	-139.7		-204.8	-19.1		-36.8

# 3.3.2 Nitrogen balance

The ensemble simulation uses nitrogen deposition as well as synthetic and organic nitrogen fertilization for the inventory simulations as input data. This data does not change between the climate change scenarios, and we, therefore, see in the ensemble results identical input fluxes for N deposition and N fertilization inputs. Nitrogen deposition from atmospheric sources contributed by 5.68 kg N ha<sup>-1</sup> yr<sup>-1</sup> on croplands (see Table 5 and Figure 5), while synthetic nitrogen fertilization was 100.88 kg N ha<sup>-1</sup> yr<sup>-1</sup> and organic nitrogen fertilization was 19.89 kg N ha<sup>-1</sup> yr<sup>-1</sup> across both scenarios and all years and rotations. In contrast, simulated biological nitrogen fixation accounted for 0.55 and 0.42 kg N ha<sup>-1</sup> yr<sup>-1</sup> for the present and future scenarios of RCP4.5, while in the RCP8.5 scenarios, the biological nitrogen fixation accounted for 0.49 and 0.27 kg N ha<sup>-1</sup> yr<sup>-1</sup> in the present and future conditions, respectively. (The crop management is based on the crop majority, such that legume crops only appear very rarely in the crop rotations, less than 2%.)

The gaseous out-fluxes that resulted from the ensemble simulations for present are  $N_2O$  emissions of 0.494 or 0.476 kg  $N_2O-N$  ha<sup>-1</sup> yr<sup>-1</sup>, NO emissions of 0.031 kg NO-N ha<sup>-1</sup> yr<sup>-1</sup>,  $N_2$  emissions of 4.806 or 4.252 kg  $N_2-N$  ha<sup>-1</sup> yr<sup>-1</sup> and  $NH_3$  emissions of 24.662 or 28.829 kg  $NH_3-N$  ha<sup>-1</sup> yr<sup>-1</sup> comparing ensemble





means versus medians in the case of RCP4.5 scenario. For the future time slice, we notice stronger differences in gaseous out-fluxes as  $N_2O$  emissions under RCP4.5 of 0.476 (mean and median) versus 0.453 or 0.457 kg  $N_2O$ –N  $ha^{-1}$  yr<sup>-1</sup> under RCP8.5.  $N_2$  emissions show a decline in the future, comparing under RCP4.5 of 4.252 or 4.354 kg  $N_2$ –N  $ha^{-1}$  yr<sup>-1</sup> versus 3.377 or 3.171 kg  $N_2$ –N  $ha^{-1}$  yr<sup>-1</sup> under RCP8.5. Ammonia volatilization and out-fluxes show a strong future increase from 28.829 or 28.069 kg NH<sub>3</sub>–N  $ha^{-1}$  yr<sup>-1</sup> to 35.040 or 34.205 kg NH<sub>3</sub>–N  $ha^{-1}$  yr<sup>-1</sup>, comparing ensemble means versus medians for RCP4.5 versus RCP8.5 climate change ensembles (compare Figure 4). Nitrate leaching is together with nitrogen removal via agricultural yields and straw the largest nitrogen flux within the system (see Figure 4). The ensemble simulations show an increase in nitrate leaching losses (comparing present to future time slices) for the mean from 54.304 to 56.049 kg  $NO_3$ -N  $ha^{-1}$  yr<sup>-1</sup> (from 50.083 to 51.421 for the median) for RCP4.5 and from 50.752 to 58.213 kg  $NO_3$ -N  $ha^{-1}$  yr<sup>-1</sup> (48.786 to 53.937 for the median) (see Figure 4). The analysis of the individual fluxes is illustrated in Figure 4.

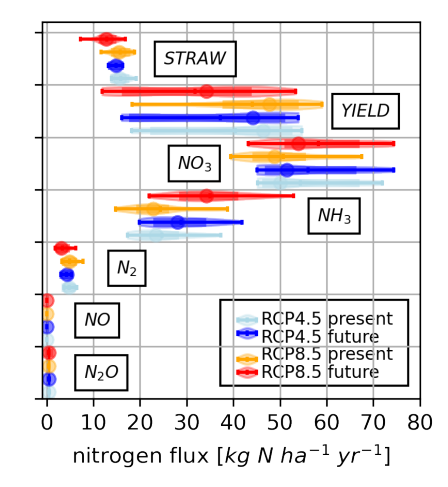


Figure 4. Violine / whisker diagram for all N outfluxes. The violin plots span the entire range; the whiskers (solid horizontal line) indicate the interquartile ranges from Q25 to Q75, while the vertical line indicates the median, and the point indicates the mean values.

Figure 5 illustrates the overall nitrogen balance (NB) in a waterfall diagram that cumulatively depicts all nitrogen out-fluxes starting with  $N_2O$  and the bottom and cumulating gaseous outfluxes in red, fluxes to open waters in blue, and N fluxes leaving the fields as yield/straw in green versus influxes (N-fertilization, manuring, BNF, and deposition) colored in brown. For each component in the NB, the associated uncertainty is illustrated as a violin representing the IQR. This diagram effectively conveys the overall soil nitrogen loss of the ensemble results as the difference between cumulative inflows and outflows. The net nitrogen loss for the period 2010-2030 results in 4.3 kg N ha<sup>-1</sup> yr<sup>-1</sup> under RCP4.5, while it equals 4.0 kg N

# https://doi.org/10.5194/egusphere-2025-5311 Preprint. Discussion started: 2 December 2025 © Author(s) 2025. CC BY 4.0 License.

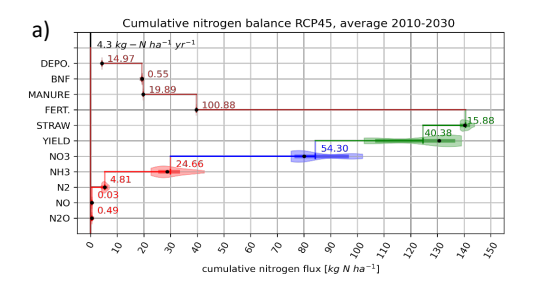


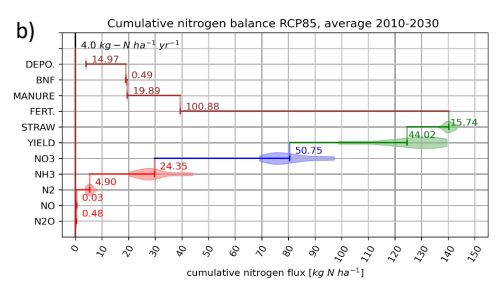


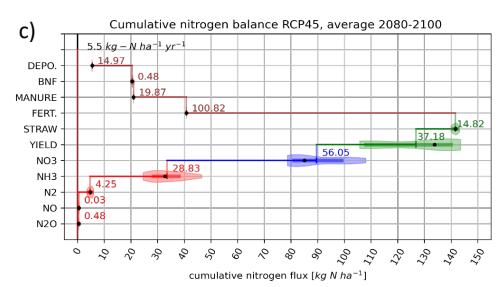
345	ha <sup>-1</sup> yr <sup>-1</sup> under RCP8.5, on a national scale. For the period 2070-2100, nitrogen loss is estimated to be 5.5
346	kg N ha <sup>-1</sup> yr <sup>-1</sup> under RCP4.5 and 5.7 kg N ha <sup>-1</sup> yr <sup>-1</sup> under RCP8.5.
347	
348	

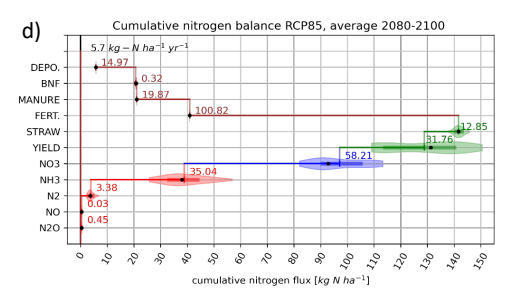












351

Figure 5. Waterfall diagram depicting the climate change impact assessment of the nitrogen balance (NB) of arable land cultivation for current (2010-2030) versus future (2080-2100) conditions under the RCP4.5 and RCP8.5 climate change scenarios. The violin plots span the entire range; the whiskers (solid horizontal line) indicate the interquartile ranges from Q25 to Q75, while the vertical line indicates the median, and the point indicates the mean values.





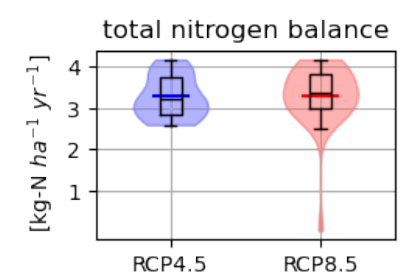


Figure 6. Distribution of the total N balances for the RCP4.5 and RCP8.5 for 2005 to 2100. Positive values indicate a net nitrogen outflux of the system. (violin plots with colored vertical bar as means, whisker plot with medians)

Table 5. Summary of the nitrogen fluxes for the present condition on a national scale and the projected rate of change, including prediction uncertainty.

Scenario	Prese	Present (2010-2030)			Future (2080-2100)			Change rate			
Scenario	[kg	g-N ha <sup>-1</sup> y	yr <sup>-1</sup> ]	[kg-N ha <sup>-1</sup> yr <sup>-1</sup> ]			[kg-N ha <sup>-1</sup> yr <sup>-1</sup> ]				
N fluxes	Mean	Std	Median	Mean	Std	Median	Mean	Std	Median		
RCP4.5											
N <sub>2</sub> O	0.494	0.033	0.498	0.476	0.037	0.476	-0.018	0.004	-0.022		
NO	0.031	0.003	0.031	0.031	0.004	0.032	0.000	0.001	0.001		
N <sub>2</sub>	4.806	0.824	4.784	4.252	0.710	4.354	-0.554	-0.114	-0.430		
NH <sub>3</sub>	24.662	5.574	23.395	28.829	6.283	28.069	4.167	0.709	4.674		
NO <sub>3</sub>	54.304	9.610	50.083	56.049	10.181	51.421	1.745	0.571	1.338		
RCP8.5											
N <sub>2</sub> O	0.479	0.027	0.480	0.453	0.037	0.457	-0.026	0.010	-0.023		
NO	0.031	0.004	0.031	0.032	0.006	0.031	0.001	0.002	0.000		
N <sub>2</sub>	4.898	1.079	4.894	3.377	1.013	3.171	-1.521	-0.066	-1.723		
NH <sub>3</sub>	24.353	6.309	22.822	35.040	7.634	34.205	10.687	1.325	11.383		
NO <sub>3</sub>	50.752	7.924	48.786	58.213	9.524	53.937	7.461	1.600	5.151		





# 3.4 Climate impact on the carbon and nitrogen cycle

# 3.4.1 Long-term dynamics

Figure 7 shows the dynamics of the ensemble simulations for the soil carbon and soil nitrogen stocks of the 30 cm topsoil (illustrated as a 10-year rolling mean).

The dynamics of the SOC show from 2050 onwards a steady decrease in SOC/loss of soil carbon stocks by approx. 11.1 kg-C ha<sup>-1</sup> yr<sup>-1</sup> for RCP4.5 and 26,7 kg-C ha<sup>-1</sup> yr<sup>-1</sup> for RCP8.5, respectively, when considering the mean across the ensemble results (Figure 7 (a)). For the RCP8.5 ensemble results mean and the median show very similar behaviour, which means that the distribution of the ensemble results is close to symmetric. For the RCP4.5, the ensemble shows non-congruent and non-uniform dynamics of the median versus the mean, which means that the ensemble result distribution is not uniform but skewed towards higher values. The dynamics of the soil nitrogen stock behave uniformly with an 13.6 averaged carbon-to-nitrogen ratio.

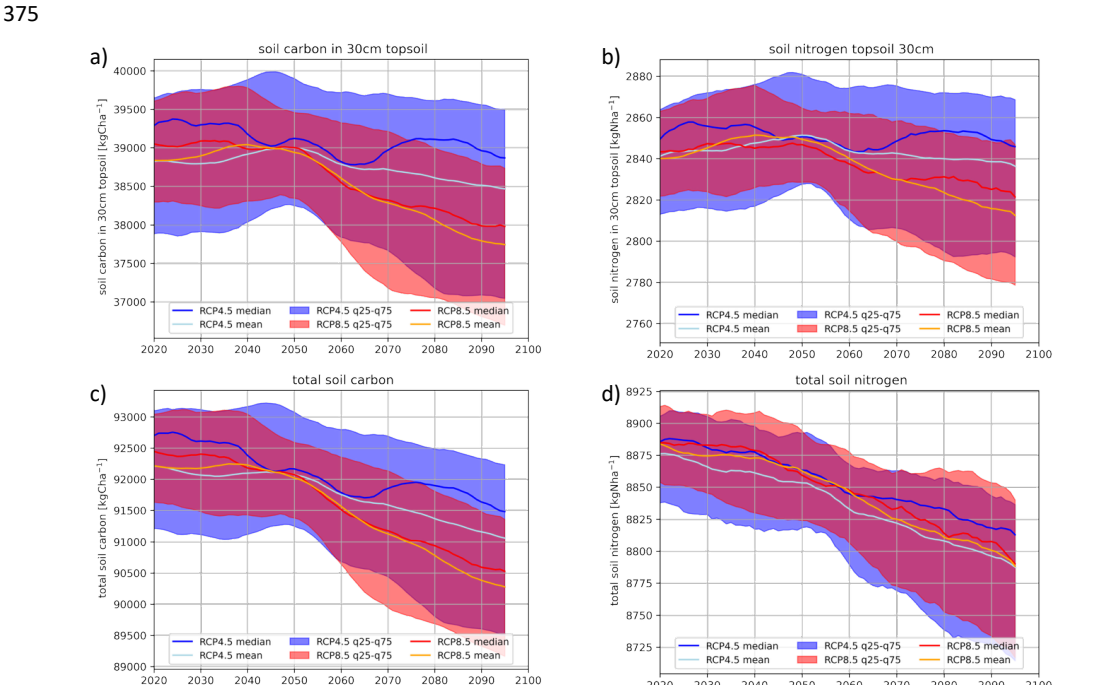


Figure 7. Dynamics of soil carbon (SC) and soil nitrogen (SN) for cropland cultivations in Greece: Dynamics of a) averaged carbon 30cm topsoil, c) total soil carbon stocks [kg-C ha<sup>-1</sup>], b) averaged 30cm topsoil, and d) total soil nitrogen stocks [kg-N ha<sup>-1</sup>].

The dynamics of the gaseous and aquatic nitrogen fluxes are shown in Figure 8, a) to e). While the NO emissions are very low, they show uniform dynamics for both climate change scenarios. The  $N_2$  emissions (from denitrification) show a rather uniform behaviour until 2060, when the ensembles of RCP4.5 deviate

# https://doi.org/10.5194/egusphere-2025-5311 Preprint. Discussion started: 2 December 2025 © Author(s) 2025. CC BY 4.0 License.





from RCP8.5. The dynamics of the N<sub>2</sub>O emissions of the ensembles behave quite uniformly, with significantly deviating dynamics of the two climate change ensembles starting around 2075 and onwards. For the ammonia emissions, the ensemble dynamics develop uniformly until around 2055, when the warmer RCP8.5 ensemble results in higher emission strength of approx. 35 kg NH<sub>3</sub>-N ha<sup>-1</sup> yr<sup>-1</sup> compared to approx. 28 kg NH<sub>3</sub>-H ha<sup>-1</sup> yr<sup>-1</sup> for RCP4.5 in 2095. The dynamics of the nitrate leaching show minor but significant differences until 2050 and a uniform behaviour towards 2100 between the ensembles.





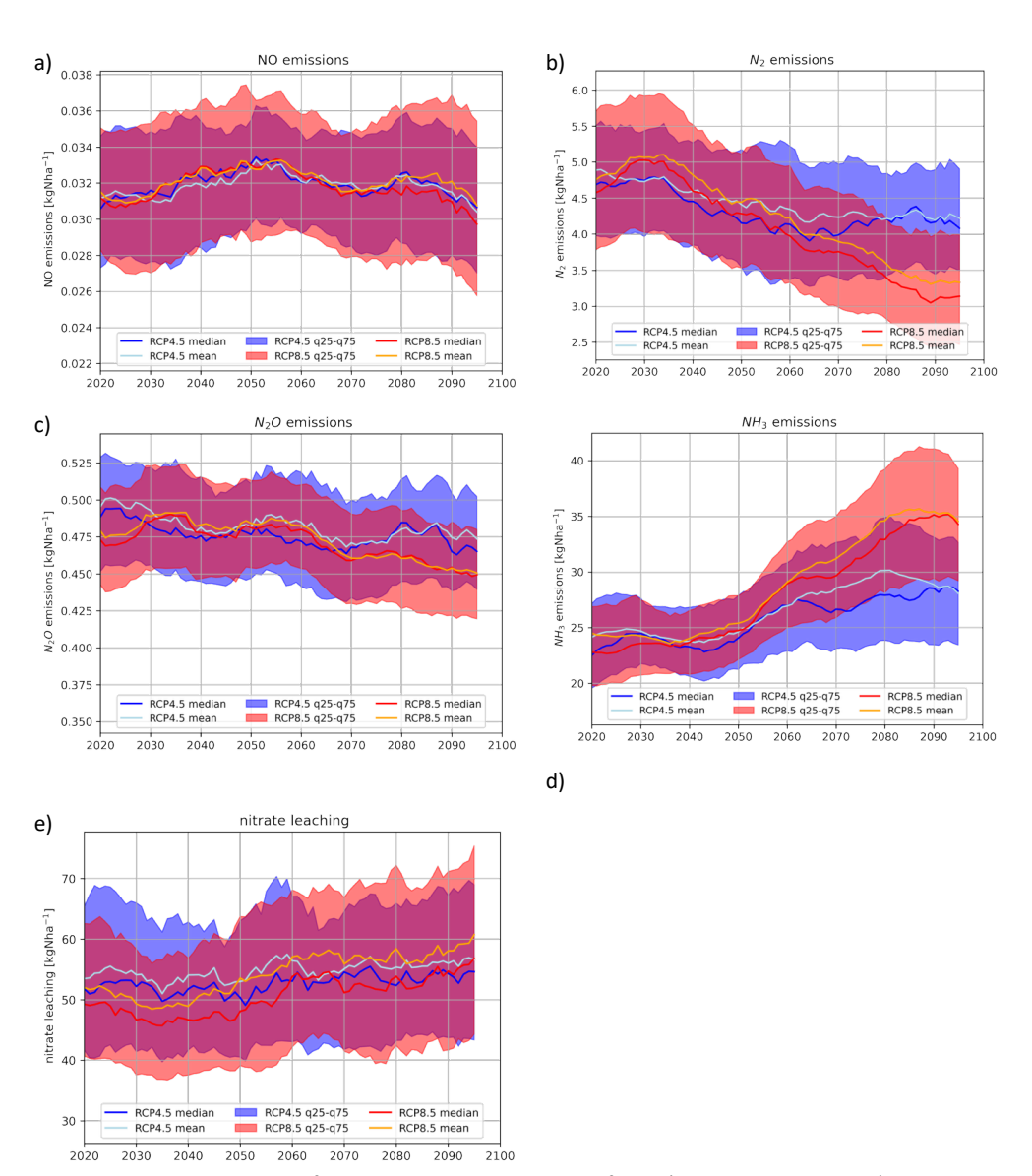


Figure 8. Temporal dynamics of gaseous and aquatic nitrogen fluxes (10-year rolling means) 2020 to 2095 for a) NO emissions; b)  $N_2$  emissions; c)  $N_2$ O emissions; d)  $NH_3$  emissions, and e) nitrate leaching losses (all fluxes in kg-N ha<sup>-1</sup> yr<sup>-1</sup>).

392393

390



395 396

397

398

399

400

401

402

403

404

405

406

407

408

409

410

411

412

413

414

415

416

417

418

419

420

421

422

423

424

425

426

427

428

429

land.



## 4 Discussion

In this study, the combined carbon and nitrogen balance of cropland agriculture is assessed for the first time on a national scale. Until now, the published reporting and assessment of the full nitrogen balance in cropland and grassland systems have been scarce and limited to a regional scale. Despite the recognized importance of such reportings and analyses highlighted by leading scientists working on nitrogen cycling in soils (Grosz et al., 2023), only Schroeck et al. (2019) reported the N balance for two alpine catchments in Austria, Sifounakis et al. (2024) reported an uncertainty analysis for the N balance for a region in Greece and Rahimi et al. (2024) reported the full N balance for 6 catchments in Denmark. Further, the concept of climate impact assessment of the C and N cycles in cropland ecosystems is introduced by propagating climate change model ensembles through an ecosystem model. It is highlighted that the large increase in temperatures within the climate change ensembles is expected to impact cropland productivity only marginally, assuming that irrigation water is still available, as it is under present conditions, and has been done in other studies (Deryng et al., 2011; Teixeira et al., 2013). We observe significant differences in our results for the present conditions in the ensemble results for RCP4.5 and RCP8.5, despite these scenarios using the same historical climate conditions until 2005 and continuing with different climate projections due to varying global CO<sub>2</sub> emission scenarios towards 2100. Olschewski et al., (2024) have shown that the ensembles exhibit a significant spread for the historical time slice of the Mediterranean region and that bias correction of the individual ensemble representations enhances their predictive quality. Similar results have been observed in our study, as well as the spread in annual mean temperature and precipitation; for example, for the year 2000, this appears to be significant. In our study, the present conditions were defined as the mean values from 2005 to 2034 and are already within the projection time slice of the EURO-CORDEX RCPs. The major observed differences across ensembles in the current conditions are primarily driven by the variations in the selected climate change projection sets from the full EURO-CORDEX ensemble. We have decided to use all the available projections for RCP4.5 and RCP8.5 to increase predictive quality into the future of the climate impact study. The selection of the sets of climate change projections used in this study was due to the availability of the datasets at the EURO-CORDEX data centers at the start of the study and their completeness to process input data for the model. The resulting mismatch was an outer constraint to the study, which we could not resolve, or rather had not anticipated at the start. We had only 14 climate data sets from common GCM/RCM combinations across the RCP4.5 and RCP8.5 scenarios, while the RCP4.5 ensemble contains 2 more datasets, and the RCP8.5 contains 18 climate datasets, unique to these scenarios. The input dataset used in this study may impose some uncertainty on the results, as the fertilization rates may be underestimated. While the total synthetic and organic nitrogen fertilization will meet national statistics, the underlying size of arable land (used to calculate the fertilization rates) may be too large due to the former land use aggregation, including unfertilized orchards, vineyards, and fallow land as arable





430 The climate change impact on crop productivity under RCP4.5 reveals a very moderate decrease towards 431 2100 in the simulation ensemble, while the IQR spread increases. This trend does not correlate with the 432 annual temperature and precipitation trend shown and is likely resulting from, e.g., changes in seasonal 433 precipitation distributions towards 2100 (data not shown). In the RCP8.5 ensembles, a statistically significant and severe decline in production starting in 2050 towards 2100 was observed, which correlates 434 435 with trends of declining annual precipitation and an increase in the precipitation IQR spread of the 436 ensemble, as seen in other studies (Bai et al., 2022; Carozzi et al., 2022; Deryng et al., 2011; Teixeira et 437 al., 2013). Some of the climate projections under RCP8.5 reveal a decline in average annual precipitation 438 from 500mm to 300mm, which will challenge agricultural production, and under such conditions, the 439 irrigation management using approx. 150mm may be unrealistic. 440 The LandscapeDNDC model, as used in this study, provides a robust plant physiological process 441 description, based on a temperature sum approachKlicken oder tippen Sie hier, um Text einzugeben. in 442 combination with water and nutrient limitation on daily growth, as well as water and heat stress, and 443 plant senescence. The model is clearly limited by the challenges imposed by climate change, such as e.g., 444 anthesis heat stress causing severe losses for various grain crops, which may occur under RCP8.5 with a 445 higher likelihood (Deryng et al., 2011; Olschewski et al., 2024; Sánchez-Benítez et al., 2022; Teixeira et al., 446 2013). On the other hand, LandscapeDNDC provides one of the most advanced soil bio-geochemical 447 processes descriptions, proving a robust prediction of soil carbon and nitrogen cycling under present and future conditions (Basche et al., 2016; Grados et al., 2024; Jägermeyr et al., 2021; Petersen et al., 2021). 448 449 Projecting current management practices into the future introduces another significant source of 450 uncertainty; however, no alternative was available due to a lack of available management projections. 451 Winter vernalization will be under pressure as it is, e.g., for winter wheat under RCP8.5, as the number of 452 chill days (vernalization) may decrease or even vanish by 2100, such that winter wheat cultivation may 453 become impossible. Although LandscapeDNDC incorporates the vernalization process, its level of 454 complexity may be insufficient to reliably estimate cereal production under extreme climate change 455 conditions by the end of the century. 456 On the other hand, climate change may shift cultivation periods and phenology completely, towards 457 winter, to avoid extreme heat stress or the introduction of multicropping seasons due to a prolongation 458 of suitable climatic conditions (Bai et al., 2022; Petersen et al., 2021). This was not a focus of this study 459 and has therefore not been investigated. The study has shown that under RCP8.5 with temperature increases and precipitation declines towards 2100, crop production will face major challenges, but will 460 still be possible even under extreme conditions, and therefore, the management conditions used in this 461 462 study remain within the possible trajectories. 463 The analysis of the soil carbon balance shows a decrease in carbon input into the system in the future due 464 to climate change, while the respiration decreases accordingly. This reveals a very moderate loss of soil 465 carbon starting in 2050 towards 2100, compared to (Basche et al., 2016; Carozzi et al., 2022). The loss



467

468

469

470

471

472

473

474

475

476

477

478

479

480

481

482

483

484 485

486

487

488

489

490

491

492

493

494

495

496

497

498

499

500

501



rates of 25 versus 30 kg C ha<sup>-1</sup> yr<sup>-1</sup> for topsoil (0-30cm) versus the total soil profile in the RCP8.5 are at the lower end of the published data and compare to the results of Haas et al. (2022) for the baseline scenarios. While Triantakonstantis et al. (2024) reported average loss rates of 1.5 t C ha<sup>-1</sup> yr<sup>-1</sup> for Greece over the past 10 years, Yigini & Panagos (2016) reported contrasting SOC increases using climate change scenarios until 2050. Lugato et al. (2014) modelled SOC dynamics until 2100 using two climate change realizations, deploying the Daycent model on LUCAS soil sampling points and upscaling to the EU-27. Our ensemble simulation results fit well with the SOC stocks for present conditions by Lugato et al. (2014), reporting, for the majority of Lucas points in Greece, topsoil C losses of similar ranges to those in our study, while some regions in Greece remain in equilibrium or achieve very small C gains until 2100. It is noticeable that the spread in simulated SOC content for the topsoil as well as the total soil profile increases towards 2100, which reflects the differences in C input (photosynthesis) and output (respiration due to decomposition) in some ensemble simulations, resulting in added uncertainty to the overall SOC estimation. On the national scale, the nitrogen outfluxes of the system are determined by the underlying management practices, and assuming a projection of this management into the future, it is clearly highlighted that for present conditions, the largest flux of nitrogen is the nitrate leaching into surface waters of approx 51 and 54 kg NO<sub>3</sub>-N ha<sup>-1</sup> yr<sup>-1</sup>, which compares well with Sifounakis et al., (2024). This corresponds to 36 or 38 % of the nitrogen input into the system and poses a substantial threat to drinking water quality on the national scale. These findings are in line with recommendations by Karyotis et al., (2002), Velthof et al., (2009) using the Miterra-Europe model or Lyra et al., (2021) reporting nitrate concentration observations in the Almyros basin under intense agricultural use. In our study, we neglected nitrate content in the irrigation water to avoid further uncertainty. We have used a static irrigation scheme by calendar day/phenology, which was projected into the future, not accounting for actual soil water content on irrigation day, irrigation water nitrogen load, and irrigation water availability due to climate change. The second largest nitrogen loss flux was ammonia volatilization to the atmosphere, driven by local conditions of slight to moderate alkalinity, with pH values of 7 and higher. The reported fluxes of 20% for present conditions, up to 30% under future conditions for alkaline soils, agree well with global estimates by Zhan et al. (2021) of 12 to 16% or Pan et al. (2016) of up to 18% of the applied fertilizers. These losses were found to increase in the future under climate change conditions due to their temperature dependence of the volatilization (Beaudor et al., 2025) supporting our findings. Shen et al., (2020) reported for U.S. cropland, that warming alone can raise agricultural NH<sub>3</sub> emissions by up to 80% by 2100, highlighting strong temperature sensitivities. These estimates indicate that the deposition scenarios used in this study, based on Haas et al., (2022) (derived from EMEP data), might underestimate the redeposition of ammonia into the landscape. The reported ammonia losses represent 17 to 18% of the total nitrogen outflux of the system. Analysing the N2O emission fluxes, our study reports rather low N2O emission fluxes compared to Sifounakis (2024), reporting N₂O emissions for the intensively cultivated region of Thessaly (Greece) of 2.6





kg N ha<sup>-1</sup> yr<sup>-1</sup> under much higher N influxes of up to 220 kg N ha<sup>-1</sup> yr<sup>-1</sup>. N₂O emission measurements for 502 503 Greece have not been reported in the literature. Carozzi et al. (2022) reported for European soils 504 estimates of 1.2 kg N ha<sup>-1</sup> yr<sup>-1</sup> (STD of 0.2) and 1.57 kg N ha<sup>-1</sup> yr<sup>-1</sup> (STD 0.2) for the cases of RCP4.5 and RCP8.5, respectively, for the first half of the century. During the second half of the century, the estimation 505 rose to 1.66 kg N ha<sup>-1</sup> yr<sup>-1</sup> (STD 0.3) and 1.93 kg N ha<sup>-1</sup> yr<sup>-1</sup> (STD 0.3) for the RCP4.5 and RCP8.5 scenarios, 506 507 while our study reveals slightly declining emission strengths towards 2100. 508 The N<sub>2</sub>O emissions in our study are lower when compared to the estimates of the latest Greek NIR 509 (Hellenic Republic Ministry of Environment and Energy, 2025), reporting N₂O emissions from cropland 510 soils of approx. 7.49 kt  $N_2O-N$  yr<sup>-1</sup> or 2.59 kg  $N_2O-N$  ha<sup>-1</sup> yr<sup>-1</sup>. 511 Regarding the N<sub>2</sub> outflux, other model studies (e.g., Sifounakis, 2024, with LandscapeDNDC in Thessaly) show  $N_2$  emissions of 15 kg  $N_2$ -N ha<sup>-1</sup> yr<sup>-1</sup> compared to approx. 4.5 kg  $N_2$ -N ha<sup>-1</sup> yr<sup>-1</sup> in our ensemble 512 inventories for present conditions, which results from higher irrigation levels fostering denitrification 513 514 upon N2O emissions. Our ensemble study observed a stronger decline in N2 versus N2O emissions towards 515 2100, which aligns with the decline in precipitation and, consequently, a decline in soil water and an 516 increase in anaerobic soil conditions that hampers denitrification and N₂ emissions. We have not analyzed 517 the dynamics of the N<sub>2</sub>:N<sub>2</sub>O relationships of each ensemble simulation. 518 The study underestimates the influence of legume crops as a nitrogen input source into the soil in Greece 519 on a national scale, due to its consideration of only four major crops in arable management. The reported 2% of the cropland 520 share of cultivated pulses in Greece is under 521 (ELSTAT: https://www.statistics.gr/en/statistics/-/publication/SPG06/2023, last access: February 2024), but (Sifounakis et al., 2024) has shown that the incorporation of legume crops as feed crops in crop 522 523 rotations in one region in Greece has a large influence on the SOC dynamics and on the overall NB. 524 Comparing the simulated Nitrogen balances for the present and future conditions, a marginal increase in 525 the yearly N deficit for the climate change ensembles is shown. Assuming an average C/N ratio of the soils 526 at 11, these nitrogen losses are larger than the corresponding SOC losses, which indicates a higher loss of 527 the soil nitrogen pools. The climate change impact on the NB is rather low when comparing future versus present conditions (change in approx. 0.2 and 1.2 kg N ha<sup>-1</sup> yr<sup>-1</sup> for RCP4.5 and RCP8.5, respectively). 528 529 The projected shifts in internal nitrogen fluxes are significant, with large declines in nitrogen harvest 530 outfluxes towards increases in NH3 volatilization and nitrate leaching losses in the future. While NH3 volatilization is temperature-driven, which impacts the equilibrium of NH<sub>4</sub> versus NH<sub>3</sub> due to Henry's law, 531 a large portion will also be attributed to reduced nitrogen uptake, resulting in reduced productivity and 532 533 more nutrients being available for physical excess pathways (volatilization/gas diffusion, and leaching). 534 It is highlighted that these results correspond to temporal and spatial averaging across the whole study 535 region, and that spatio-temporal patterns have not been considered in the analysis. Furthermore, it is underlined that the ensemble results between RCP4.5 and RCP8.5 must be compared with caution, as 536 537 each of these ensembles has been constructed with a different number and types of GCM/RCM





simulations, with the RCP8.5 scenario being significantly more populated compared to RCP4.5. At the beginning of the study, it was expected that a larger number of ensemble members would be beneficial and might increase the overall prediction quality. Our advice for future studies is to reduce uncertainty and always try to use sets of GCM/RCM projections across all analysed climate change scenarios. In that context, it is emphasized that the differences between the RCP scenarios are distinctively identified already for the present and near future conditions, when the underlying socioeconomic assumptions of each RCP start to influence. The EURO-CORDEX climate change ensembles claim to be bias-adjusted for the European conditions (ECMWF homepage), but large variations within the ensembles have been noticed for Greece, already for the historical period, which concludes that for such regions it is advised to perform local bias corrections as suggested by Olschewski et al. (2024). Menz (2023) has published bias-corrected EURO-CORDEX Data for 8 RCMs and is expected to have a reduced spread in the ensembles, while newer CMIP6 (Eyring et al., 2016) climate change projections are becoming available, with the split from historic to climate projection being closer to the present.

# 5 Conclusion

Ensembles of EURO-CORDEX climate change projections (RCP4.5 and RCP8.5) were propagated through the bio-geochemical process model LandscapeDNDC to assess the impacts on the carbon and nitrogen cycling and the associated GHG emissions from arable soils on a national scale for Greece. For the present time slice, the study presents for the first time a national-scale inventory of the full carbon and nitrogen balance of the Greek arable land cultivation from a process-based ecosystem model.

While the climate change ensembles show expected behaviour towards 2100 for Greece, such as a steady

While the climate change ensembles show expected behaviour towards 2100 for Greece, such as a steady increase in surface temperature (median 1.35 °C for RCP4.5, 3.30°C for RCP8.5 over land), arable production will only decline substantially under RCP8.5 towards 2100, while predicted changes in precipitation are less recognisable.

The projected changes in the carbon and nitrogen balance, and their related excess outfluxes towards the end of the century, were relatively small. Despite pronounced annual warming, simulated soil carbon stocks remained stable, defying anticipated declines from temperature-driven mineralization.

The study outperforms the few previous climate impact assessments, which have mostly examined only one single flux, relied on a single climate projection, or reported results for individual sites rather than regional or national inventories.

To increase prediction reliability and reduce uncertainty, some aspects may have to be considered in future assessments:









600	Projections in the North China Plain. Frontiers in Plant Science, 13.
601	https://doi.org/10.3389/fpls.2022.829580
602	Basche, A. D., Archontoulis, S. V., Kaspar, T. C., Jaynes, D. B., Parkin, T. B., & Miguez, F. E. (2016). Simulating
603	long-term impacts of cover crops and climate change on crop production and environmental
604	outcomes in the Midwestern United States. <i>Agriculture, Ecosystems and Environment, 218,</i> 95–106.
605	https://doi.org/10.1016/j.agee.2015.11.011
606	Beaudor, M., Vuichard, N., Lathière, J., & Hauglustaine, D. A. (2025). Future Trends of Global Agricultural
607	Emissions of Ammonia in a Changing Climate. Journal of Advances in Modeling Earth Systems, 17(4).
608	https://doi.org/10.1029/2023MS004186
609	Bojinski, S., Verstraete, M., Peterson, T. C., Richter, C., Simmons, A., & Zemp, M. (2014). The concept of
610	essential climate variables in support of climate research, applications, and policy. Bulletin of the
611	American Meteorological Society, 95(9), 1431–1443. https://doi.org/10.1175/BAMS-D-13-00047.1
612	Carozzi, M., Martin, R., Klumpp, K., & Massad, R. S. (2022). Effects of climate change in European croplands
613	and grasslands: Productivity, greenhouse gas balance and soil carbon storage. Biogeosciences,
614	19(12), 3021–3050. https://doi.org/10.5194/bg-19-3021-2022
615	Deryng, D., Sacks, W. J., Barford, C. C., & Ramankutty, N. (2011). Simulating the effects of climate and
616	agricultural management practices on global crop yield. Global Biogeochemical Cycles, 25(2), n/a-
617	n/a. https://doi.org/10.1029/2009gb003765
618	Eden, J. M., Widmann, M., Grawe, D., & Rast, S. (2012). Skill, correction, and downscaling of GCM-
619	simulated precipitation. Journal of Climate, 25(11), 3970–3984. https://doi.org/10.1175/JCLI-D-11-
620	00254.1
621	ESDB. (2004). European Soil Database (ESDB) v2.0 - raster version.
622	https://esdac.jrc.ec.europa.eu/ESDB_Archive/ESDB/ESDB_Data/ESDB_v2_data_smu_1k.html
623	Eyring, V., Bony, S., Meehl, G. A., Senior, C. A., Stevens, B., Stouffer, R. J., & Taylor, K. E. (2016). Overview
624	of the Coupled Model Intercomparison Project Phase 6 (CMIP6) experimental design and
625	organization. Geoscientific Model Development, 9(5), 1937–1958. https://doi.org/10.5194/gmd-9-
626	1937-2016
627	Giorgi, F. (2006). Climate change hot-spots. <i>Geophysical Research Letters</i> , 33(8).
628	https://doi.org/10.1029/2006GL025734
629	Grados, D., Kraus, D., Haas, E., Butterbach-Bahl, K., Olesen, J. E., & Abalos, D. (2024). Common agronomic
630	adaptation strategies to climate change may increase soil greenhouse gas emission in Northern
631	Europe. Agricultural and Forest Meteorology, 349.
632	https://doi.org/10.1016/j.agrformet.2024.109966
633	Grosz, B. P., Matson, A., Butterbach-Bahl, K., Clough, T., Davidson, E. A., Dechow, R., & Scheer, C. (2023).
634	Modeling denitrification: can we report what we don't know? AGU Advances - ESS Open Archive .
635	https://doi.org/10.22541/essoar.168500283.32887682/v1





636 Haas, E., Carozzi, M., Massad, R. S., Butterbach-Bahl, K., & Scheer, C. (2022). Long term impact of residue 637 management on soil organic carbon stocks and nitrous oxide emissions from European croplands. 638 Science of The Total Environment, 836, 154932. https://doi.org/10.1016/J.SCITOTENV.2022.154932 639 Haas, E., Klatt, S., Fröhlich, A., Kraft, P., Werner, C., Kiese, R., Grote, R., Breuer, L., & Butterbach-Bahl, K. 640 (2013). LandscapeDNDC: A process model for simulation of biosphere-atmosphere-hydrosphere 641 exchange processes at site and regional scale. Landscape Ecology, 28(4), 615-636. 642 https://doi.org/10.1007/s10980-012-9772-x 643 Hellenic Republic Ministry of Environment and Energy. (2025). CLIMATE CHANGE NATIONAL INVENTORY 644 REPORT OF GREECE FOR GREENHOUSE AND OTHER GASES FOR THE YEARS 1990-2023 NATIONAL 645 INVENTORY DOCUMENT. https://ypen.gov.gr/wp-content/uploads/2025/04/2025\_NIR\_Greece.pdf 646 Jacob, D., Teichmann, C., Sobolowski, S., Katragkou, E., Anders, I., Belda, M., Benestad, R., Boberg, F., 647 Buonomo, E., Cardoso, R. M., Casanueva, A., Christensen, O. B., Christensen, J. H., Coppola, E., De 648 Cruz, L., Davin, E. L., Dobler, A., Domínguez, M., Fealy, R., ... Wulfmeyer, V. (2020). Regional climate 649 downscaling over Europe: perspectives from the EURO-CORDEX community. Regional Environmental 650 Change, 20(2). https://doi.org/10.1007/s10113-020-01606-9 651 Jägermeyr, J., Müller, C., Ruane, A. C., Elliott, J., Balkovic, J., Castillo, O., Faye, B., Foster, I., Folberth, C., 652 Franke, J. A., Fuchs, K., Guarin, J. R., Heinke, J., Hoogenboom, G., Iizumi, T., Jain, A. K., Kelly, D., Khabarov, N., Lange, S., ... Rosenzweig, C. (2021). Climate impacts on global agriculture emerge 653 earlier in new generation of climate and crop models. Nature Food, 2(11), 873-885. 654 655 https://doi.org/10.1038/s43016-021-00400-y 656 Karyotis, Th., Panagopoulos, A., Pateras, D., Panoras, A., Danalatos, N., Angelakis, C., & Kosmas, C. (2002). 657 The Greek Action Plan for the mitigation of nitrates in water resources of the vulnerable district of 658 Thessaly. Journal of Mediterranean Ecology, 3(2-3), 77-83. 659 Kraus, D., Weller, S., Klatt, S., Haas, E., Wassmann, R., Kiese, R., & Butterbach-Bahl, K. (2014). A new 660 LandscapeDNDC biogeochemical module to predict CH4 and N2O emissions from lowland rice and 661 upland cropping systems. Plant and Soil, 386(1-2), 125-149. https://doi.org/10.1007/s11104-014-662 2255-x 663 Li, C. S. (2000). Modeling trace gas emissions from agricultural ecosystems. Nutrient Cycling in 664 Agroecosystems, 58(1-3), 259-276. https://doi.org/10.1023/A:1009859006242 Lugato, E., Bampa, F., Panagos, P., Montanarella, L., & Jones, A. (2014). Potential carbon sequestration of 665 European arable soils estimated by modelling a comprehensive set of management practices. Global 666 667 Change Biology, 20(11), 3557-3567. https://doi.org/10.1111/gcb.12551 668 Lyra, A., Loukas, A., & Sidiropoulos, P. (2021). Impacts of irrigation and nitrate fertilization scenarios on 669 groundwater resources quantity and quality of the Almyros Basin, Greece. Water Supply, 21(6), 670 2748-2759. https://doi.org/10.2166/ws.2021.097





671 Menz, C. (2023). Bias Adjusted CORDEX-EUR11 Simulations. World Data Center for Climate (WDCC) at 672 DKRZ. https://doi.org/10.26050/WDCC/BAdCORD-EUR11 673 Nocentini, A., Di Virgilio, N., & Monti, A. (2015). Model Simulation of Cumulative Carbon Sequestration by Switchgrass (Panicum Virgatum L.) in the Mediterranean Area Using the DAYCENT Model. Bioenergy 674 675 Research, 8(4), 1512-1522. https://doi.org/10.1007/s12155-015-9672-4 676 Olschewski, P., Dieng, M. D. B., Moutahir, H., Böker, B., Haas, E., Kunstmann, H., & Laux, P. (2024). 677 Amplified potential for vegetation stress under climate-change-induced intensifying compound 678 extreme events in the Greater Mediterranean Region. Natural Hazards and Earth System Sciences, 679 24(4), 1099-1134. https://doi.org/10.5194/nhess-24-1099-2024 680 Paeth, H., Schönbein, D., Keupp, L., Abel, D., Bangelesa, F., Baumann, M., Büdel, C., Hartmann, C., Kneisel, 681 C., Kobs, K., Krause, J., Krech, M., Pollinger, F., Schäfer, C., Steininger, M., Terhorst, B., Ullmann, T., Wilde, M., Ziegler, K., ... Hotho, A. (2023). Climate change information tailored to the agricultural 682 683 sector in Central Europe, exemplified on the region of Lower Franconia. Climatic Change, 176(10). 684 https://doi.org/10.1007/s10584-023-03613-1 685 Pan, B., Lam, S. K., Mosier, A., Luo, Y., & Chen, D. (2016). Ammonia volatilization from synthetic fertilizers 686 and its mitigation strategies: A global synthesis. Agriculture, Ecosystems and Environment, 232, 283-687 289. https://doi.org/10.1016/j.agee.2016.08.019 688 Petersen, K., Kraus, D., Calanca, P., Semenov, M. A., Butterbach-Bahl, K., & Kiese, R. (2021). Dynamic 689 simulation of management events for assessing impacts of climate change on pre-alpine grassland 690 productivity. European Journal Agronomy, 128, 126306. 691 https://doi.org/https://doi.org/10.1016/j.eja.2021.126306 692 Portmann, F. T., Siebert, S., & Döll, P. (2010). MIRCA2000-Global monthly irrigated and rainfed crop areas 693 around the year 2000: A new high-resolution data set for agricultural and hydrological modeling. 694 Global Biogeochemical Cycles, 24(1), n/a-n/a. https://doi.org/10.1029/2008gb003435 695 Rahimi, J., Haas, E., Scheer, C., Grados, D., Abalos, D., Aderele, M. O., Blicher-Mathiesen, G., & Butterbach-696 Bahl, K. (2024). Aggregation of activity data on crop management can induce large uncertainties in 697 of regional estimates nitrogen budgets. Npj Sustainable Agriculture, 2(1). 698 https://doi.org/10.1038/s44264-024-00015-3 699 Sánchez-Benítez, A., Goessling, H., Pithan, F., Semmler, T., & Jung, T. (2022). The July 2019 European Heat 700 Wave in a Warmer Climate: Storyline Scenarios with a Coupled Model Using Spectral Nudging. 701 American Meteorological Society, 35(8), 2373-2390. https://doi.org/10.1175/JCLI-D-21 702 Schroeck, A. M., Gaube, V., Haas, E., & Winiwarter, W. (2019). Estimating nitrogen flows of agricultural 703 soils at a landscape level - A modelling study of the Upper Enns Valley, a long-term socio-ecological 704 research region in Austria. Science of the Total Environment, 665, 705 https://doi.org/10.1016/j.scitotenv.2019.02.071





706	Shen, H., Chen, Y., Hu, Y., Ran, L., Lam, S. K., Pavur, G. K., Zhou, F., Pleim, J. E., & Russell, A. G. (2020).
707	Intense Warming Will Significantly Increase Cropland Ammonia Volatilization Threatening Food
708	Security and Ecosystem Health. One Earth, 3(1), 126–134.
709	https://doi.org/10.1016/j.oneear.2020.06.015
710	Sifounakis, O., Haas, E., Butterbach-Bahl, K., & Papadopoulou, M. P. (2024). Regional assessment and
711	uncertainty analysis of carbon and nitrogen balances at cropland scale using the ecosystem model
712	LandscapeDNDC. Biogeosciences, 21(6), 1563–1581. https://doi.org/10.5194/bg-21-1563-2024
713	Sperna Weiland, F. C., Visser, R. D., Greve, P., Bisselink, B., Brunner, L., & Weerts, A. H. (2021). Estimating
714	Regionalized Hydrological Impacts of Climate Change Over Europe by Performance-Based Weighting
715	of CORDEX Projections. Frontiers in Water, 3. https://doi.org/10.3389/frwa.2021.713537
716	Teixeira, E. I., Fischer, G., Van Velthuizen, H., Walter, C., & Ewert, F. (2013). Global hot-spots of heat stress
717	on agricultural crops due to climate change. Agricultural and Forest Meteorology, 170, 206–215.
718	https://doi.org/10.1016/j.agrformet.2011.09.002
719	Triantakonstantis, D., Batsalia, M., & Lolos, N. (2024). Spatio-Temporal Dynamics of Soil Organic Carbon
720	Stock in Greek Croplands: A Long-Term Assessment. Sustainability (Switzerland), 16(18).
721	https://doi.org/10.3390/su16187984
722	Velthof, G. L., Oudendag, D., Witzke, H. P., Asman, W. A. H., Klimont, Z., & Oenema, O. (2009). Integrated
723	Assessment of Nitrogen Losses from Agriculture in EU-27 using MITERRA-EUROPE. Journal of
724	Environmental Quality, 38(2), 402–417. https://doi.org/10.2134/jeq2008.0108
725	Wilby, R. L., & Dessai, S. (2010). Robust adaptation to climate change. Weather, 65(7), 180–185.
726	https://doi.org/https://doi.org/10.1002/wea.543
727	Yang, Z., & Villarini, G. (2021). Evaluation of the capability of global climate models in reproducing the
728	temporal clustering in heavy precipitation over Europe. International Journal of Climatology, 41(1),
729	131–145. https://doi.org/10.1002/joc.6612
730	Yigini, Y., & Panagos, P. (2016). Assessment of soil organic carbon stocks under future climate and land
731	cover changes in Europe. Science of the Total Environment, 557–558, 838–850.
732	https://doi.org/10.1016/j.scitotenv.2016.03.085
733	Zhan, X., Adalibieke, W., Cui, X., Winiwarter, W., Reis, S., Zhang, L., Bai, Z., Wang, Q., Huang, W., & Zhou,
734	F. (2021). Improved Estimates of Ammonia Emissions from Global Croplands. <i>Environmental Science</i>
735	and Technology, 55(2), 1329–1338. https://doi.org/10.1021/acs.est.0c05149
736	
737	